

Hole spin relaxation in Ge-Si core-shell nanowire qubits

Yongjie Hu^{1,2†}, Ferdinand Kuemmeth², Charles M. Lieber^{1,3*} and Charles M. Marcus^{2*}

Controlling decoherence is the biggest challenge in efforts to develop quantum information hardware^{1–3}. Single electron spins in gallium arsenide are a leading candidate among implementations of solid-state quantum bits, but their strong coupling to nuclear spins produces high decoherence rates^{4–6}. Group IV semiconductors, on the other hand, have relatively low nuclear spin densities, making them an attractive platform for spin quantum bits. However, device fabrication remains a challenge, particularly with respect to the control of materials and interfaces⁷. Here, we demonstrate state preparation, pulsed gate control and charge-sensing spin readout of hole spins confined in a Ge-Si core-shell nanowire. With fast gating, we measure T_1 spin relaxation times of up to 0.6 ms in coupled quantum dots at zero magnetic field. Relaxation time increases as the magnetic field is reduced, which is consistent with a spin-orbit mechanism that is usually masked by hyperfine contributions.

Since the proposal of Loss and DiVincenzo's¹, the promise of quantum dots for solid-state quantum computation has been underscored by the successful initialization, manipulation and readout of electron spins in GaAs systems^{5,8–10}. The electronic wavefunctions in these systems typically overlap with a large number of nuclear spins that are difficult to control and in most cases thermally randomized. The resulting intrinsic spin decoherence rates^{4–6} have been successfully reduced by spin-echo techniques^{6,11}, but require complex gate sequences that complicate multi-qubit operations¹². The prospect of achieving long coherence times in group IV materials with few nuclear spins has stimulated many proposals^{13,14} and intensive experimental efforts^{15–19}, and crucially depends on the development of high-quality host materials. Recent advances regarding single quantum dots have been achieved using Zeeman splitting for readout with a finite magnetic field^{19–23}. Coupled quantum-dot devices^{13,15–18,24} in a nuclear spin-free system are more desirable for flexible quantum manipulation²⁵ but more challenging, and characterization of the spin lifetime has yet to be completed.

Semiconductor nanowires form a favourable platform for quantum devices because of the ability to precisely control their diameter, composition, morphology and electronic properties during synthesis²⁶. The prototypical Ge-Si nanowire heterostructure has revealed diverse phenomena at the nanoscale and enabled numerous applications in nanoelectronics. The epitaxial growth of silicon around a single-crystal germanium core (Fig. 1, inset) and the associated valence band offset provide a natural radial confinement of holes that, due to the large sub-band spacing, behave one-dimensionally at low temperature²⁷. Although the topmost valence band has been predicted to be twofold degenerate and of light-hole character under idealized approximations²⁸, it is generally expected that mixing between heavy and light hole bands due to

confinement will affect spin relaxation through phonons and spin-orbit interaction. To assess the potential of holes in Ge-Si heterostructure nanowires for spintronic applications we directly probed the spin relaxation times in top-gate defined quantum dots.

Our spin qubit device (Fig. 1) consists of a double quantum dot and a charge sensor that is electrically insulated but capacitively coupled to the double dot by means of a floating gate (green). The double dot is defined by barriers in the nanowire induced by positive voltages applied to gates L, M and R (blue). Plunger gates

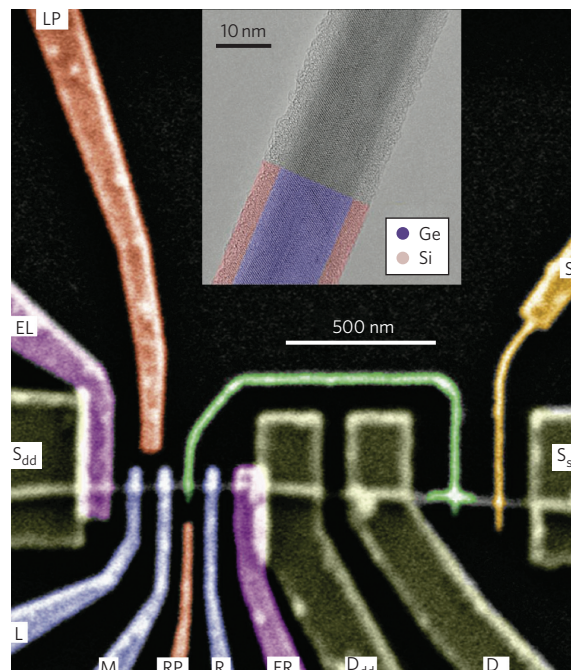
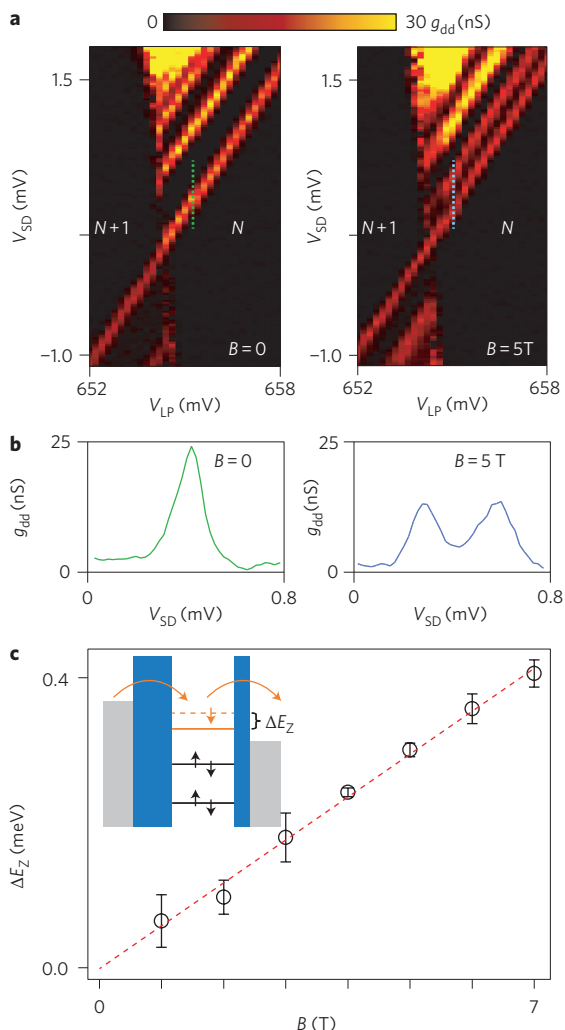


Figure 1 | Spin qubit device based on a Ge-Si heterostructure nanowire. Scanning electron micrograph (with false colour) of a Ge-Si nanowire (horizontal) contacted by four palladium contacts (S_{dd} , D_{dd} , S_s , D_s , grey) and covered by a HfO_2 gate dielectric layer. Top gates L, M and R (blue) induce a double quantum dot on the left device. Plunger gates LP and RP (orange) change the chemical potential of each dot independently, and side gates EL and ER (purple) improve electrical contact to the nanowire. A single quantum dot on the right half of the nanowire (isolated by chemical etching between D_{dd} and D_s) is capacitively coupled to a floating gate (green) and a tuning gate (yellow), and senses the charge state of the double dot. Inset: transmission electron microscope image of a typical nanowire with a single-crystal germanium core and an epitaxial silicon shell.

¹Department of Chemistry and Chemical Biology, Harvard University, Cambridge, Massachusetts 02138, USA; ²Department of Physics, Harvard University, Cambridge, Massachusetts 02138, USA; ³School of Engineering and Applied Sciences, Harvard University, Cambridge, Massachusetts 02138, USA;

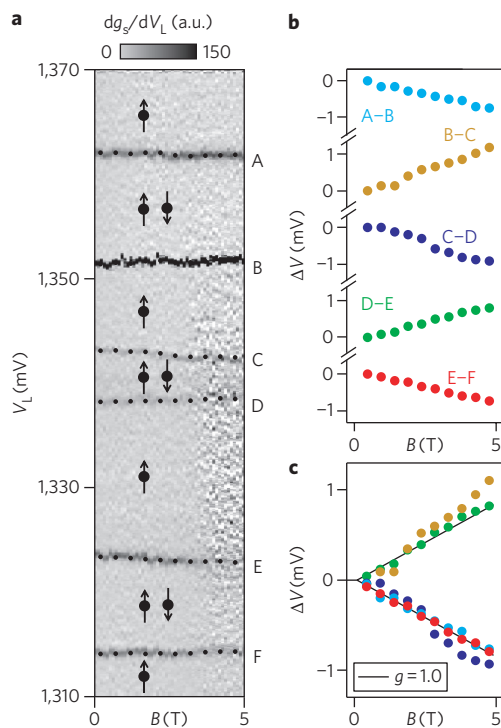
†Present address: Department of Mechanical Engineering, Massachusetts Institute of Technology, Cambridge, Massachusetts, 02139, USA.

*e-mail: cml@cmliris.harvard.edu; marcus@harvard.edu



LP and RP (orange) tune the energy levels of each dot and gates EL and ER (purple) increase the carrier densities near the source (S_{dd}) and drain (D_{dd}) to provide efficient charge transmission between nanowire and contacts. A tuning gate S (yellow) operates the sensor dot near a Coulomb oscillation where the sensor conductance g_s (measured by $\sim 30 \mu\text{V}_{\text{rms}}$ excitation standard locking techniques) is most sensitive to the potential of the floating gate.

We first performed transport spectroscopy in a single quantum dot defined by top gates L and M, while leaving all other gate electrodes at smaller gate voltages to allow hole flow through the nanowire. Investigating the differential conductance $g_{dd} = dI/dV_{SD}$ as a function of bias V_{SD} and gate voltage V_{LP} (Fig. 2a) revealed Coulomb diamonds and the excitation spectrum of the dot. The data show a set of conductance lines parallel to the diamond edge due to tunnelling through asymmetric barriers into excited quantum states (Fig. 2c, inset). First, we note that for $V_{SD} > 0$ the lowest excited state appears $\sim 0.6 \text{ meV}$ above the ground-state resonance. Such a high level spacing constitutes an advantage for spin qubits where the lowest spin states need to be addressed



without occupation of higher orbitals. Second, a finite magnetic field splits the spin-degenerate ground-state transition into a spin-up and spin-down resonance (Fig. 2b). Their separation allows us to extract the Zeeman energy $E_Z = |g|\mu_B B$, where g is the g -factor and $\mu_B = 5.8 \times 10^{-5} \text{ eV T}^{-1}$ is the Bohr magneton. A linear fit to Zeeman splittings at different magnetic fields (Fig. 2c, $g \approx 1.02$) yields a g -factor that is significantly smaller than that of unperturbed light holes in germanium ($|g_{||}| \approx 2|\kappa| \approx 2 \times 3.41 = 6.82$)^{28,29}, probably due to strong confinement and heavy-hole light-hole mixing. Although $g \neq 2$ provides indirect evidence for the presence of spin-orbit coupling, the observed twofold spin degeneracy is consistent with recent experiments on holes in germanium and silicon quantum dots^{19,20,30,31}. Note that in the absence of external or internal (that is, nuclear) magnetic fields, hole states with half-integer total angular momentum are expected to be (at least) twofold degenerate due to time-reversal symmetry, so it is natural to create spin qubits from such Kramers doublets, in close analogy to the singlet-triplet qubits of two-electron spin states.

To form a double quantum dot in the spin-blockade regime²⁵, we raised the barriers and lowered the hole density by tuning the gate voltages. The number of holes in each dot was estimated to be between 10 and 50. In this regime, we verify the even-odd filling of spin-degenerate ground states using the charge sensor described previously¹⁶. Figure 3a shows the sensing data of six subsequent charge transitions of the double dot, visible as discrete peaks in the differential sensor dot conductance dg_s/dV_L . With increasing magnetic field the transitions increase or decrease in energy (gate voltage), depending on the direction of the added hole spin. To clarify this field dependence we plotted the voltage spacing ΔV

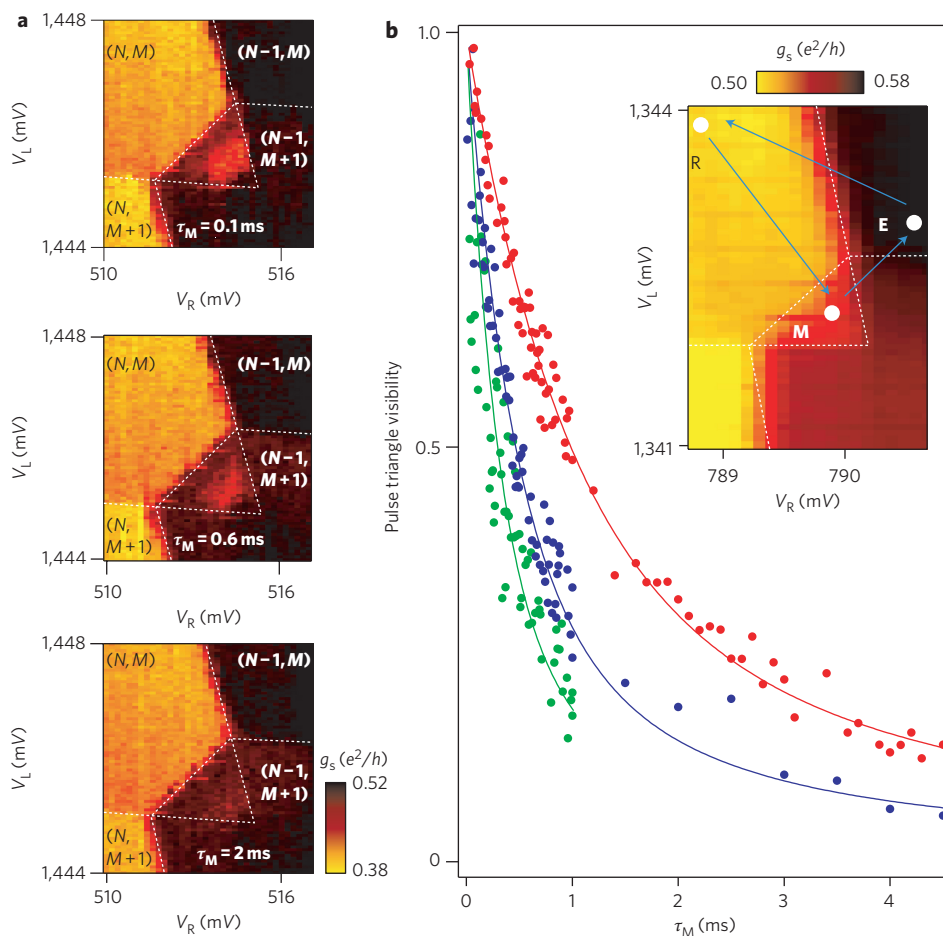


Figure 4 | Pulsed gate measurements of spin relaxation times. **a**, Sensor conductance g_s near a spin-blocked charge transition between the left and right dot. Spin-to-charge conversion results in pulse triangles that fade away with increasing measurement time τ_M . Here, N and M indicate an odd number of holes in the left and right dots (denoted (1,1) in the main text). **b**, Visibility $I(\tau_M)$ measured at the centre of the pulse triangle versus τ_M at different magnetic fields. The fitting curves (solid lines) give $T_1 = 0.6, 0.3$ and 0.2 ms at $B = 0$ (red), 0.1 (blue) and 1 T (green), respectively. Inset: blue arrows visualize the T_1 pulse sequence in gate voltage space when the measurement point is held in the centre of the pulse triangle.

between consecutive peaks, reduced by their spacing near zero field (Fig. 3b). Assuming that the coupling efficiency of gate L is close to that extracted from Fig. 2a, we find that the ground-state magnetic moments are consistent with $g = 1.0$ (Fig. 3c, solid line). The alternating sign of the magnetic moments reflects the even–odd filling of spin-degenerate hole states in the double dot. To simplify the following discussion we denote odd occupation of both dots as (1,1) and even occupation as (0,2), similar to singlet–triplet qubits in few-electron double dots²⁵. Moreover, for sufficiently large orbital level spacing, the ground state of (0,2) is singly degenerate (all spins in each dot are paired, ‘singlet’), whereas (1,1) additionally allows parallel alignment of the two unpaired spins (‘triplets’).

Next, we characterized hole spin relaxation by realizing spin-to-charge conversion in a cyclic gate-pulse sequence $E \rightarrow R \rightarrow M \rightarrow E$ (Fig. 4b, inset) that was continuously repeated while measuring g_s as a function of gate voltages V_L and V_R . As 80% of the cycle period is spent at the measurement point (M), the time-averaged sensor conductance reflects the charge state of the double dot during the measurement time τ_M . Starting with the left dot empty, (0,1), the pulse sequence resets the (1,1) double dot during R to either a triplet or singlet state by tunnelling a hole of random spin state through the left barrier. An adiabatic gate pulse to M converts only the (1,1) singlet state to the (0,2) charge configuration. States with parallel hole spins remain in the (1,1) charge configuration due to Pauli exclusion, thereby increasing

the sensor conductance g_s within the metastable region outlined by a white dotted triangle. Within this pulse triangle, g_s takes values between (1,1) and (0,2), characterized by the visibility $I = [g_s(\tau_M) - g_s(\infty)]/[g_s(0) - g_s(\infty)]$. With increasing measurement time, spin relaxation processes from the spin-blocked (1,1) charge configuration into the (0,2) ground state are more likely to occur, resulting in a decay of the visibility with increasing τ_M (Fig. 4a). By fitting the measured visibility in the centre of the pulse triangle by⁵

$$I(\tau_M) = (\tau_M)^{-1} \int_0^{\tau_M} e^{-t/T_1} dt$$

we extract a spin relaxation time of $T_1 \approx 0.6$ ms at $B = 0$ (Fig. 4b). At all measurement points, we observed no pulse triangle when the cycle was reversed ($R \rightarrow E \rightarrow M \rightarrow R$), demonstrating that the asymmetric inter-dot tunnelling was dominated by Pauli blockade.

The extracted relaxation time T_1 decreases with increasing magnetic field to 0.3 ms and 0.2 ms at $B = 0.1$ and 1 T respectively (Fig. 4b). This weak dependence is qualitatively consistent with spin relaxation via a spin-orbit interaction³² and two-phonon processes³³, but may also reflect relaxation through Coulomb coupling with electrons in the gates³⁴. Additional work remains to illuminate the relaxation mechanism in detail, but we note that recent

experiments in silicon and Si/SiO₂ interfaces have observed a clear power-law dependence only at high magnetic fields (several tesla)^{21,23,35}. Based on the split-off band in bulk germanium (0.29 eV, compared to 0.38 eV in InAs (ref. 36)), we speculate that the spin-orbit coupling is of comparable strength^{14,37} to that in InAs nanowire qubits³⁸ and, in conjunction with heavy/light hole mixing, may allow rapid electrical spin manipulation techniques that are absent in electron-based qubits, such as rapid direct spin rotation³⁹ and a recently predicted direct Rashba spin-orbit interaction¹⁴.

In summary, we have observed spin doublets of holes confined in one-dimensional Ge–Si nanowires. We have observed Pauli blockade in the double dot regime and achieved a spin qubit with long spin relaxation time of ~0.6 ms at zero field. The characterization of spin states and spin lifetime presented here underscores the potential of heterostructure nanowires as a platform for coherent spintronics that will not suffer from fluctuating polarizations of nuclear spins and will take advantage of electrical control.

Methods

The Ge–Si core–shell heterostructure nanowires were synthesized by a nanocluster-catalysed methodology as described previously¹⁶ and predominantly exhibit a ⟨110⟩ growth direction. The germanium core diameter could be controlled between 10 and 20 nm by the choice of gold catalyst, and the epitaxial silicon shell thickness between 2 and 5 nm. Devices were fabricated on a degenerately doped silicon substrate with 600 nm thermal oxide that was grounded during measurements. Electrical contact to the nanowire was established by means of source-drain electrodes patterned by electron-beam lithography from a thermally evaporated film of palladium (30 nm). The entire chip was then covered by a 10 nm thin layer of HfO₂ (dielectric constant, ~23) using atomic layer deposition. HfO₂ was deposited at 200 °C in 100 cycles of 1 s water vapour pulse, 5 s N₂ purge, 3 s precursor and 5 s N₂ purge. Tetrakis (dimethylamino) hafnium [Hf(N(CH₃)₂)₄] was used as precursor. Electron-beam lithography was used to define the top gates, followed by thermal evaporation of aluminium (50 nm). The device was measured in a ³He refrigerator with a base temperature of 280 mK, and a magnetic field was applied along the axis of the nanowire with an accuracy of 30°. A Tektronix AWG520 pulse generator was used to apply fast voltages to gates L and R through low-temperature bias-tees, resulting in a rise time of 3 ns.

Received 30 September 2011; accepted 21 November 2011;
published online 18 December 2011

References

- Loss, D. & DiVincenzo, D. P. Quantum computation with quantum dots. *Phys. Rev. A* **57**, 120–126 (1998).
- Hanson, R. & Awschalom, D. Coherent manipulation of single spins in semiconductors. *Nature* **453**, 1043–1049 (2008).
- Petta, J. R., Lu, H. & Gossard, A. C. A coherent beam splitter for electronic spin states. *Science* **327**, 669–672 (2010).
- Khaetskii, A. V., Loss, D. & Glazman, L. Electron spin decoherence in quantum dots due to interaction with nuclei. *Phys. Rev. Lett.* **88**, 186802 (2002).
- Johnson, A. *et al.* Triplet–singlet spin relaxation via nuclei in a double quantum dot. *Nature* **435**, 925–928 (2005).
- Petta, J. *et al.* Coherent manipulation of coupled electron spins in semiconductor quantum dots. *Science* **309**, 2180–2184 (2005).
- Dyakonov, M. I. (ed.) *Spin Physics in Semiconductors* (Springer Series in Solid-State Sciences 157, Springer, 2008).
- Elzerman, J. M. *et al.* Single-shot read-out of an individual electron spin in a quantum dot. *Nature* **430**, 431–435 (2004).
- Koppens, F., Buizert, C., Tielrooij, K. & Vink, I. Driven coherent oscillations of a single electron spin in a quantum dot. *Nature* **442**, 766–771 (2006).
- Nowack, K., Koppens, F. & Nazarov, Y. Coherent control of a single electron spin with electric fields. *Science* **318**, 1430–1433 (2007).
- Bluhm, H. *et al.* Dephasing time of GaAs electron-spin qubits coupled to a nuclear bath exceeding 200 μs. *Nature Phys.* **7**, 109–113 (2011).
- Foletti, S., Bluhm, H., Mahalu, D., Umansky, V. & Yacoby, A. Universal quantum control of two-electron spin quantum bits using dynamic nuclear polarization. *Nature Phys.* **5**, 903–908 (2009).
- Trauzettel, B., Bulavik, D. V., Loss, D. & Burkard, G. Spin qubits in graphene quantum dots. *Nature Phys.* **3**, 192–196 (2007).
- Kloeffel, C., Trif, M. & Loss, D. Strong spin-orbit interaction and helical hole states in Ge/Si nanowires. *Phys. Rev. B* **84**, 195314 (2011).
- Mason, N., Bieruk, M. & Marcus, C. Local gate control of a carbon nanotube double quantum dot. *Science* **303**, 655–658 (2004).
- Hu, Y. *et al.* A Ge/Si heterostructure nanowire-based double quantum dot with integrated charge sensor. *Nature Nanotech.* **2**, 622–625 (2007).
- Steele, G. A., Gotz, G. & Kouwenhoven, L. P. Tunable few-electron double quantum dots and Klein tunnelling in ultraclean carbon nanotubes. *Nature Nanotech.* **4**, 363–367 (2009).
- Shaji, N. *et al.* Spin blockade and lifetime-enhanced transport in a few-electron Si/SiGe double quantum dot. *Nature Phys.* **4**, 540–544 (2008).
- Katsaros, G. *et al.* Hybrid superconductor–semiconductor devices made from self-assembled SiGe nanocrystals on silicon. *Nature Nanotech.* **5**, 458–464 (2010).
- Zwanenburg, F. A., van Rijmenam, C., Fang, Y., Lieber, C. M. & Kouwenhoven, L. P. Spin states of the first four holes in a silicon nanowire quantum dot. *Nano Lett.* **9**, 1071–1079 (2009).
- Xiao, M., House, M. G. & Jiang, H. W. Measurement of the spin relaxation time of single electrons in a silicon metal-oxide–semiconductor-based quantum dot. *Phys. Rev. Lett.* **104**, 096801 (2010).
- Simmons, C. B. *et al.* Tunable spin loading and *T*₁ of a silicon spin qubit measured by single-shot readout. *Phys. Rev. Lett.* **106**, 156804 (2011).
- Hayes, R. R. *et al.* Lifetime measurements *T*₁ of electron spins in Si/SiGe quantum dots. Preprint at arXiv:0908.0173v1 (2009).
- Borselli, M. G. *et al.* Pauli spin blockade in undoped Si/SiGe two-electron quantum dots. *Appl. Phys. Lett.* **99**, 063109 (2011).
- Hanson, R., Petta, J. R., Tarucha, S. & Vandersypen, L. M. K. Spins in few-electron quantum dots. *Rev. Mod. Phys.* **79**, 1217–1265 (2007).
- Lieber, C. & Wang, Z. Functional nanowires. *MRS Bull.* **32**, 99–108 (2007).
- Lu, W., Xiang, J., Timko, B., Wu, Y. & Lieber, C. One-dimensional hole gas in germanium/silicon nanowire heterostructures. *Proc. Natl Acad. Sci. USA* **102**, 10046–10051 (2005).
- Zulicke, U. & Csontos, D. Zeeman splitting in cylindrical hole quantum wires. *Curr. Appl. Phys.* **8**, 237–240 (2008).
- Nenashev, A. V., DVurechenskii, A. V. & Zinov'eva, A. F. Wave functions and g factor of holes in Ge/Si quantum dots. *Phys. Rev. B* **67**, 205301 (2003).
- Zhong, Z. H., Fang, Y., Lu, W. & Lieber, C. M. Coherent single charge transport in molecular-scale silicon nanowires. *Nano Lett.* **5**, 1143–1146 (2005).
- Roddaro, S. *et al.* Spin states of holes in Ge/Si nanowire quantum dots. *Phys. Rev. Lett.* **101**, 186802 (2008).
- Wang, L., Shen, K., Sun, B. Y. & Wu, M. W. Singlet–triplet relaxation in multivalley silicon single quantum dots. *Phys. Rev. B* **81**, 235326 (2010).
- Trif, M., Simon, P. & Loss, D. Relaxation of hole spins in quantum dots via two-phonon processes. *Phys. Rev. Lett.* **103**, 106601 (2009).
- Levitov, L. S. & Rashba, E. I. Dynamical spin–electric coupling in a quantum dot. *Phys. Rev. B* **67**, 115324 (2003).
- Shankar, S., Tyryshkin, A., He, J. & Lyon, S. Spin relaxation and coherence times for electrons at the Si/SiO₂ interface. *Phys. Rev. B* **82**, 195323 (2010).
- Winkler, R. in *Spin–Orbit Coupling Effects in Two-Dimensional Electron and Hole Systems* Ch. 3, 28 (Springer Tracts in Modern Physics 191, Springer, 2003).
- Hao, X. J. *et al.* Strong and tunable spin–orbit coupling of one-dimensional holes in Ge/Si core–shell nanowires. *Nano Lett.* **10**, 2956–2960 (2010).
- Nadj-Perge, S., Frolov, S. M., Bakkers, E. P. A. M. & Kouwenhoven, L. P. Spin–orbit qubit in a semiconductor nanowire. *Nature* **468**, 1084–1087 (2010).
- Tang, J.-M., Levy, J. & Flatté, M. E. All-electrical control of single ion spins in a semiconductor. *Phys. Rev. Lett.* **97**, 106803 (2006).

Acknowledgements

The authors thank H. Churchill, J. Medford and E. Rashba for technical help and discussions, and acknowledge support from the DARPA/QuEST programme.

Author contributions

Y.H. and F.K. performed the experiments. Y.H. prepared the materials and fabricated the devices. Y.H., F.K., C.M.L. and C.M.M. analysed the data and co-wrote the paper. All authors discussed the results and commented on the manuscript.

Additional information

The authors declare no competing financial interests. Reprints and permission information is available online at <http://www.nature.com/reprints>. Correspondence and requests for materials should be addressed to C.M.L. and C.M.M.